Dynamic response of an interface crack between magnetoelectroelastic and functionally graded elastic layers

Keqiang Hu[1,*], Zengtao Chen[1], Jiawei Fu[1,2]

[1] Department of Mechanical Engineering, University of New Brunswick, Fredericton, NB, E3B 5A3, Canada
[2] Department of Mechanical Engineering, Nanjing University of Science and Technology, Nanjing 210094 China
* Corresponding author: keqianghu@163.com

Abstract The dynamic response of an interface crack between magnetoelectroelastic and functionally graded elastic layers under anti-plane shear and in-plane electric and magnetic impacts is investigated by the integral transform method. The mixed boundary value problem of the interface crack is reduced to dual integral equations, which can be further expressed in terms of a Fredholm integral equation of the second kind. The singular stress fields near the crack tip are obtained asymptotically, and the stress intensity factor (SIF) is defined. Based on the criterion of maximum hoop stress, the crack will propagate along the original crack plane and won’t kink. Numerical results show that the dynamic SIF is influenced by the material properties and geometric size ratios.

Keywords Dynamic response, Interface crack, Magnetoelctroelastic layer, Functionally graded elastic layer, Stress intensity factor

1. Introduction

Composites made of piezoelectric/piezomagnetic materials exhibit magnetoelectric effect that is not present in single-phase piezoelectric or piezomagnetic materials. Studies on the properties of piezoelectric/piezomagnetic composites have been carried out by numerous researchers [1, 2]. In particular, there is a growing interest among researchers in solving fracture mechanic problems in media possessing coupled piezoelectric, piezomagnetic and magnetoelectric effects, that is, magnetoelectroelastic effects. The crack initiation behavior in magnetoelectroelastic composite under in-plane deformation was investigated by Song and Sih [3]. Gao et al. [4] presented some exact treatments on the crack problems in magnetoelectroelastic solids. Wang and Mai [5] considered the mode III crack problems in an infinite piezoelectromagnetic medium using complex variable technique. Qin [6] obtained two dimensional (2D) Green’s functions of defective magnetoelectroelastic solids under thermal loading, which can be used to establish boundary formulation and to analyze relevant fracture problems. Li [7] made the transient analysis of a cracked magnetoelectroelastic medium under antiplane mechanical and inplane electric and magnetic impacts. Hu and Li [8] studied the crack in a magnetoelectroelastic strip under longitudinal shear. A moving crack problem in magnetoelectroelastic materials has been solved by Hu and Li [9]. Interface crack moving along dissimilar magnetoelectroelastic materials has been studied by Hu et al. [10], and Zhong and Li [11], respectively. The dynamic response of a penny-shaped crack in a magnetoelectroelastic layer was studied by Feng et al., [12]. Boundary element method was developed by Rojas-Díaz et al., [13] to study crack problems in linear magnetoelectroelastic materials under static loading conditions. The transient anti-plane problem of a magnetoelectroelastic strip containing a crack is considered by Yong and Zhou [14]. An anti-plane shear crack in a magnetoelectroelastic layer sandwiched between dissimilar half spaces has been investigated by Hu et al. [15]. Zhou and Chen [16] analyzed a partially conducting mode I crack in a piezoelectromagnetic material. Wang and Han [17] studied the effect of interfacial cracks on the magnetoelectric coupling properties of a magneto-electro-elastic composite laminate. Recently, Hu and Chen [18] conducted the pre-curving analysis of a crack in a magnetoelctroelastic strip under in-plane dynamic loading and the same authors [19] also studied the anti-plane problem of a magnetoelectroelastic strip sandwiched between elastic layers. Wan et al. [20] investigated a mode III crack crossing the magnetoelectroelastic bimaterial interface under concentrated magnetoelectromechanical loads.

The objective of this paper is to study an interface crack between magnetoelectroelastic and functionally graded elastic layers under anti-plane shear and in-plane electric and magnetic impact loading. Fourier and Laplace transforms are applied to reduce the mixed-boundary-value problem to dual integral equations, which can be further expressed in terms of a Fredholm integral equation. The stress intensity factors are obtained and the effect of geometric size and material properties are analyzed.

2. Basic equations

Consider a transversely isotropic, linear magnetoelectroelastic material. Suppose the Cartesian coordinates $x,\ y,\ z$ are the principal axes of the material symmetry, and the poling direction is oriented in the z –axis. Consider only the out-of-plane displacement, the in-plane electric field and in-plane magnetic field, i.e.,

$$u_x = u_y = 0, \quad u_z = u_z(x,y,t) \tag{1}$$

$$E_x = E_x(x,y,t), \quad E_y = E_y(x,y,t), \quad E_z = 0 \tag{2}$$

$$M_x = M_x(x,y,t), \quad M_y = M_y(x,y,t), \quad M_z = 0 \tag{3}$$

$$u_x^e = u_y^e = 0, \quad u_z^e = u_z^e(x,y,t) \tag{4}$$

where u_i, E_i and M_i $(i = x, y, z)$ are components of displacement, electrical field and magnetic field, respectively; the superscript “*e*” denotes the quantities of the elastic layers.

The constitutive equations for magnetoelectroelastic materials and elastic materials under anti-plane shear take the forms as:

$$\begin{pmatrix}\sigma_{zy}\\ D_y\\ B_y\end{pmatrix} = \begin{pmatrix}c_{44} & e_{15} & h_{15}\\ e_{15} & -\lambda_{11} & -\beta_{11}\\ h_{15} & -\beta_{11} & -\gamma_{11}\end{pmatrix}\begin{pmatrix}\dfrac{\partial u_z}{\partial y}\\ \dfrac{\partial \phi}{\partial y}\\ \dfrac{\partial \varphi}{\partial y}\end{pmatrix}, \quad \begin{pmatrix}\sigma_{zx}\\ D_x\\ B_x\end{pmatrix} = \begin{pmatrix}c_{44} & e_{15} & h_{15}\\ e_{15} & -\lambda_{11} & -\beta_{11}\\ h_{15} & -\beta_{11} & -\gamma_{11}\end{pmatrix}\begin{pmatrix}\dfrac{\partial u_z}{\partial x}\\ \dfrac{\partial \phi}{\partial x}\\ \dfrac{\partial \varphi}{\partial x}\end{pmatrix} \tag{5}$$

$$\sigma_{zy}^e = c_{44}^e \frac{\partial u_z^e}{\partial y}, \quad \sigma_{zx}^e = c_{44}^e \frac{\partial u_z^e}{\partial x} \tag{6}$$

where σ_{zj}, D_j and B_j ($j = x, y$) are components of stress, electrical displacement and magnetic induction; c_{44}, e_{15}, h_{15} and β_{11} are elastic, piezoelectric, piezomagnetic and electromagnetic constants; λ_{11} and γ_{11} are dielectric permitivity and magnetic permeability; ϕ and φ are electric potential and magnetic potential, respectively.

By introducing two new functions Φ and Ψ as [9]

$$\Phi = \phi + mu_z = \phi + \frac{\beta_{11}h_{15} - \gamma_{11}e_{15}}{\lambda_{11}\gamma_{11} - \beta_{11}^2}u_z, \quad \Psi = \varphi + nu_z = \varphi + \frac{\beta_{11}e_{15} - \lambda_{11}h_{15}}{\lambda_{11}\gamma_{11} - \beta_{11}^2}u_z \tag{7}$$

The dynamic equilibrium equations can be obtained as

$$\nabla^2 u_z = \left(\partial^2 u_z / \partial t^2\right)/V^2, \quad \nabla^2\Phi = 0, \quad \nabla^2\Psi = 0 \tag{8}$$

$$V = \sqrt{\mu/\rho}, \quad \mu = c_{44} + \left(\gamma_{11}e_{15}^2 + \lambda_{11}h_{15}^2 - 2\beta_{11}e_{15}h_{15}\right)/\left(\lambda_{11}\gamma_{11} - \beta_{11}^2\right) \tag{9}$$

where $\nabla^2 = \partial^2/\partial x^2 + \partial^2/\partial y^2$ is the two-dimensional Laplacian operator and V, μ, and ρ are the speed of the magnetoelectroelastic shear wave, the magnetoelectroelastic stiffened elastic constant, and the mass density of the magnetoelectroelastic material, respectively.

3. Problem formulation

Now let us consider an interface crack of length $2c$ between a magnetoelectroelastic layer **(M)** and a functionally graded elastic layer **(F)**, as shown in Fig. 1. The composite structure is under anti-plane shear and in-plane electric and magnetic impacts, and the thickness of the magnetoelectroelastic and functionally graded elastic layer are h_1 and h_2, respectively. Due to symmetry in geometry and loading conditions, it is sufficient to consider the problem for $0 \le x < \infty,\ -h_2 \le y \le h_1$ only.

The material properties of the functionally graded elastic layer vary continuously along the y-direction in the form as

$$c_{44}^e = c_{44}^{e0} \cdot \exp(\beta y), \quad \rho^e = \rho^{e0} \cdot \exp(\beta y) \qquad (0 \le y \le h_1) \tag{10}$$

where β is a constant and the superscript “0” denotes the material properties of the functionally graded elastic layer at the plane $y = 0$, i.e., c_{44}^{e0} and ρ^{e0} are the elastic constant and the material density of the functionally graded elastic layer at the plane $y = 0$, respectively.

The governing equation for the functionally graded elastic layer under anti-plane deformation can be obtained as:

$$\nabla^2 u_z^e + \beta\frac{\partial u_z^e}{\partial y} = \frac{1}{V_0^2}\frac{\partial^2 u_z^e}{\partial t^2} \tag{11}$$

where $V_0 = \sqrt{c_{44}^{e0}/\rho^{e0}}$ is the speed of the elastic shear wave induced by the functionally graded elastic layer.

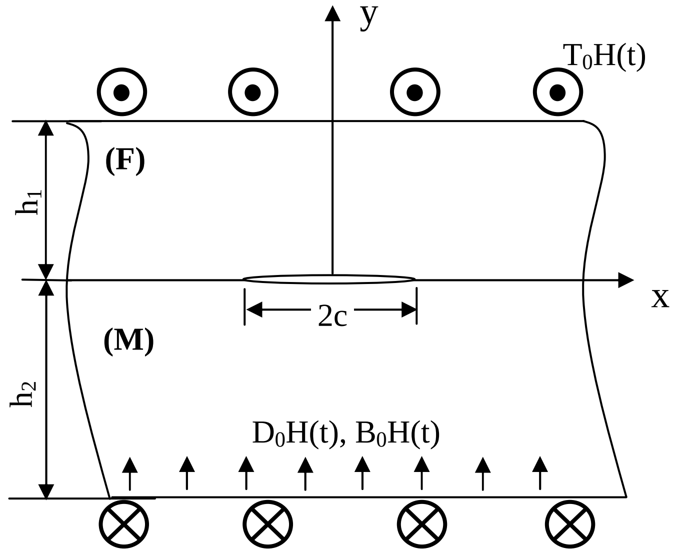

Figure 1. An interface crack between magnetoelectroelastic and functionally graded elastic layers

The electrical and magnetic boundary conditions on the edges of the magnetoelectroelastic layer are considered as follows:

$$D_y(x,0,t) = D_y(x,-h_2,t) = D_0 H(t), \quad B_y(x,0,t) = B_y(x,-h_2,t) = B_0 H(t) \tag{12}$$

where D_0 and B_0 are uniform electric displacement and magnetic induction applied on the magnetoelectroelastic layer, $H(t)$ is the Heaviside step function, $H(t)=0$ for $t<0$, and $H(t)=1$ for $t \geq 0$.

The mechanical boundary conditions are:

$$\sigma_{zy}(x,0,t) = \sigma_{zy}^{e}(x,0,t) = 0 \, , \qquad (0 \leq x < c) \tag{13}$$

$$u_z(x,0,t) = u_z^{e}(x,0,t) \, , \qquad (x \geq c) \tag{14}$$

$$\sigma_{zy}^{e}(x,h_1,t) = \sigma_{zy}(x,-h_2,t) = T_0 H(t) \qquad (x \geq 0) \tag{15}$$

$$\sigma_{zy}(x,0,t) = \sigma_{zy}^{e}(x,0,t) \, , \qquad (x \geq c) \tag{16}$$

where T_0 is the uniform shear stress.

4. Derivation of the integral equations

Appropriate solutions of Eq. (8) and Eq. (11) in the Laplace transform domain may be expressed as

$$u_z^{e*}(x,y,p)=\frac{2}{\pi}\int_0^\infty[A_1(s,p)\exp(k_1y)+A_2(s,p)\exp(k_2y)]\cos(sx)ds \\ +a_0[\exp(-\beta y)-1]/p \tag{17}$$

$$u_z^*(x,y,p)=\frac{2}{\pi}\int_0^\infty[B_1(s,p)\exp(ky)+B_2(s,p)\exp(-ky)]\cos(sx)ds+b_0\frac{y}{p} \tag{18}$$

$$\phi^*(x,y,p)=\frac{2}{\pi}\int_0^\infty[C_1(s,p)\exp(sy)+C_2(s,p)\exp(-sy)]\cos(sx)ds+c_0\frac{y}{p} \\ -\frac{2}{\pi}m\int_0^\infty[B_1(s,p)\exp(ky)+B_2(s,p)\exp(-ky)]\cos(sx)ds-mb_0\frac{y}{p} \tag{19}$$

$$\varphi^*(x,y,p)=\frac{2}{\pi}\int_0^\infty[D_1(s,p)\exp(sy)+D_2(s,p)\exp(-sy)]\cos(sx)ds+d_0\frac{y}{p} \\ -\frac{2}{\pi}n\int_0^\infty[B_1(s,p)\exp(ky)+B_2(s,p)\exp(-ky)]\cos(sx)ds-nb_0\frac{y}{p} \tag{20}$$

where p is the Laplace transform parameter, $A_j(s,p)$, $B_j(s,p)$, $C_j(s,p)$ and $D_j(s,p)$ ($j=1,\ 2$) are the unknown functions to be solved and a_0, b_0, c_0 and d_0 are real constants determined by considering the boundary and interface conditions as

$$a_0=-T_0/(c_{44}^{e0}\beta) \\ \begin{pmatrix} b_0 \\ c_0 \\ d_0 \end{pmatrix}=\begin{pmatrix} \mu & e_{15} & h_{15} \\ 0 & \lambda_{11} & \beta_{11} \\ 0 & \beta_{11} & \gamma_{11} \end{pmatrix}^{-1}\begin{pmatrix} T_0 \\ -D_0 \\ -B_0 \end{pmatrix} \tag{21}$$

and the parameters k and k_1, k_2 are defined as

$$k=\sqrt{s^2+p^2/V^2},\ \ k_{1,2}=\left[-\beta\pm\sqrt{\beta^2+4(s^2+p^2/V_0^2)}\right]/2 \tag{22}$$

A simple calculation leads to the expressions for the stresses as

$$\sigma_{zy}^{e*}=T_0/p+\frac{2}{\pi}c_{44}^e\int_0^\infty[k_1A_1(s,p)\exp(k_1y)+k_2A_2(s,p)\exp(k_2y)]\cos(sx)ds \tag{23}$$

$$\sigma_{zy}^*=T_0/p+\frac{2}{\pi}\int_0^\infty k\mu[B_1(s,p)\exp(ky)-B_2(s,p)\exp(-ky)]\cos(sx)ds \\ +\frac{2}{\pi}\int_0^\infty e_{15}s[C_1(s,p)\exp(sy)-C_2(s,p)\exp(-sy)]\cos(sx)ds \\ +\frac{2}{\pi}h_{15}\int_0^\infty h_{15}s[D_1(s,p)\exp(sy)-D_2(s,p)\exp(-sy)]\cos(sx)ds \tag{24}$$

From the boundary conditions (12), (15) and (16), there is only one independent unknown function (say $B_1(s,p)$). The following dual integral equations can be obtained from the mixed boundary conditions in Eqs. (13, 14) as

$$\int_0^\infty k\mu[1-\exp(-2kh_2)]B_1(s,p)\cos(sx)ds = -\frac{\pi T_0}{2p}, \quad (0 \le x < c) \tag{25}$$

$$\int_0^\infty F(s,p)B_1(s)\cos(sx)ds = 0, \qquad (x \ge c) \tag{26}$$

where function $F(s,p)$ is defined as

$$F(s,p) = 1+\exp(-2kh_2) + \frac{k\mu[1-\exp(-2kh_2)]\{k_2\exp[(k_2-k_1)h_1]-k_1\}}{c_{44}^{e0}k_1k_2\{1-\exp[(k_2-k_1)h_1]\}} \tag{27}$$

The dual integral equations can be solved by introducing auxiliary functions $\Phi(x,p)$ as

$$B_1(s,p) = -\frac{\pi(\mu+c_{44}^{e0})T_0}{2c_{44}^{e0}\mu p F(s,p)}c^2\int_0^1 x\Phi(x,p)J_0(scx)dx \tag{28}$$

where $J_0(\ )$ is the zero-order Bessel function of the first kind, and the function $\Phi(x,p)$ satisfies the Fredholm integral equations of the second kind

$$\Phi(x,p) + \int_0^1 \Phi(\eta,p)Q(\eta,x,p)d\eta = 1 \tag{29}$$

where the kernel functions $Q(\eta,x,p)$ is defined as

$$Q(\eta,x,p) = \eta\int_0^\infty s[R(s/c,p)-1]J_0(sx)J_0(s\eta)ds \tag{30}$$

where

$$R(s,p) = \frac{k(c_{44}^{e0}+\mu)[1-\exp(-2kh_2)]}{c_{44}^{e0}sF(s,p)} \tag{31}$$

5. Field intensities

Once functions $\Phi(x,p)$ is obtained by solving the Fredholm integral equations of the second kind Eq. (30), the singular stress fields near the crack tip in the Laplace domain can be obtained asymptotically as

$$\sigma_{zy}^*(r,\theta,p) + i\sigma_{zx}^*(r,\theta,p) = \exp(-i\theta/2)K^{T*}(p)\big/\sqrt{2\pi r} \tag{32}$$

where r and θ are defined as

$$r = \sqrt{(x-c)^2+y^2}, \quad \theta = \tan^{-1}[y/(x-c)] \tag{33}$$

the stress intensity factor (SIF) K^{T*} is defined as

$$K^{T*}(p) = \lim_{r\to 0^+}\sqrt{2\pi r}\sigma_{zy}^*(r,0,p) = T_0\Phi(1,p)\sqrt{\pi c}\big/p \tag{34}$$

The stress intensity factor in the time domain can be expressed as

$$K^T(t) = T_0\sqrt{\pi c}\Big/2\pi i\int_{Br}\exp(pt)\Phi(1,p)\big/p\,dp \tag{35}$$

where "*Br*" stands for the Bromwich path of integration. It should be noted that the stress intensity factor is only dependent on the mechanical loading, as seen from Eqs. (34), (35) and (27)-(31).

The dynamic hoop stress around the crack tip can be obtained as

$$\sigma_{z\theta}(r,\theta,t) = K^T(t)\Big/\sqrt{2\pi r}\cos(\theta/2) \qquad (-\pi \le \theta \le \pi) \tag{36}$$

It is clear that the maximum hoop stress always appears at the direction $\theta = 0^{\circ}$, which means that if the fracture toughness of the material is same in all directions, the crack will propagate along the original crack plane and no crack kinking should appear.

6. Numerical results and discussions

The material properties of the magnetoelectroelastic layer are taken as [21]

$$\begin{aligned}
&c_{44} = 5.0\times10^{10}\ (\mathrm{N/m^2}),\quad e_{15} = 0.2\ (\mathrm{C/m^2}),\quad h_{15} = 180\ (\mathrm{N/Am})\\
&\lambda_{11} = 2.5\times10^{-10}\ (\mathrm{C^2/Nm^2}),\quad \gamma_{11} = -2.0\times10^{-6}\ (\mathrm{Ns^2/C^2})\\
&\beta_{11} = 5.3\times10^{-9}\ (\mathrm{Ns/VC}),\quad \rho = 5.7\times10^{3}\ (\mathrm{Kg/m^3})
\end{aligned} \tag{37}$$

Fig. 2 shows the variation of the normalized dynamic SIFs K_T versus normalized time for different values of functionally graded material parameter β when $V = V_e$ and $h_1/c = h_2/c \to \infty$. The SIFs increase as the dimensionless time increases and reach the peak points at about $tV/c = 2.1$ and oscillate about their static values. As $tV/c \to \infty$, the dynamic SIFs appoach their static values. The magnitudes of the SIFs decrease as the functionally graded material parameter β increases from negative to positive value. Fig. 3 displays the normalized dynamic SIFs K_T vs normalized time for different values of geometric size ratio $h_1/c = h_2/c$ when $\beta = +1$ and $V = V_e$. It needs more time for the cracked composite with smaller size ratio $h_1/c = h_2/c$ to reach the stabilized values of K_T. The second peak value of the dynamic SIF seems to increase and appear earlier when the geometric size ratio $h_1/c = h_2/c$ decreases. Fig. 4 shows the normalized dynamic SIFs K_T vs normalized time for different material property

$R = c_{44}^{e0}/\mu$ when $\beta = +1$, $\rho = \rho^{e0}$ and $h_1/c = h_2/c \to \infty$. The increase of the ratio $R = c_{44}^{e0}/\mu$ will lead to the larger peak values of the dynamic SIFs as well as larger corresponding static values.

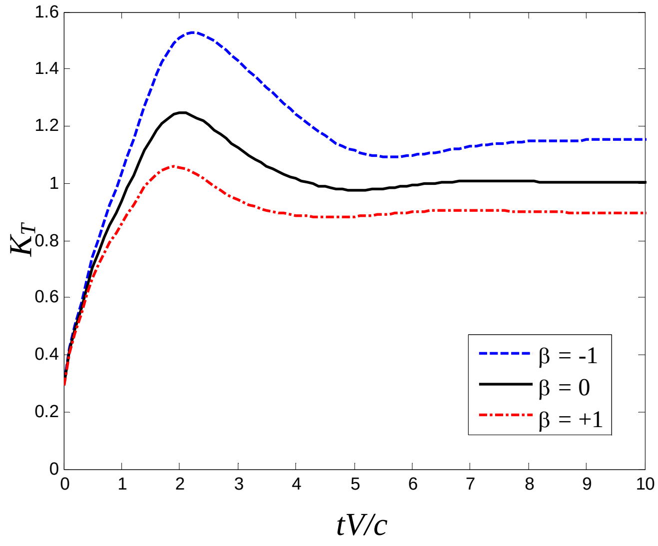

Figure 2. Normalized dynamic SIFs K_T vs normalized time for different functionally graded material parameter β when $V = V_e$

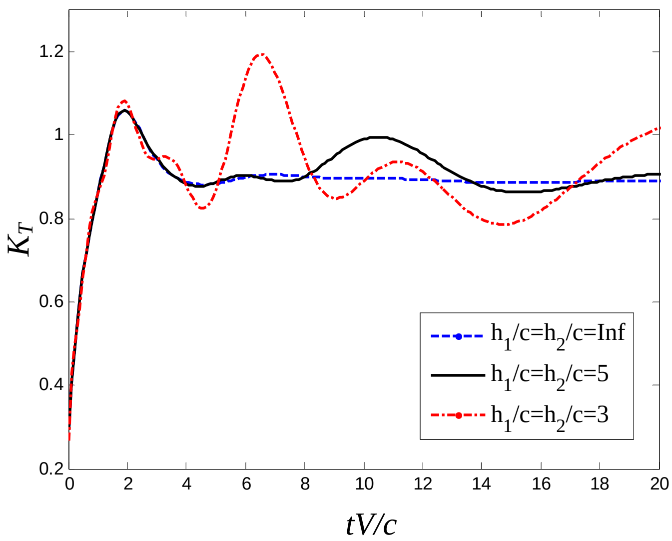

Figure 3. Normalized dynamic SIFs K_T vs normalized time for different geometric size $h_1/c = h_2/c$ when $\beta = +1$, $V = V_e$

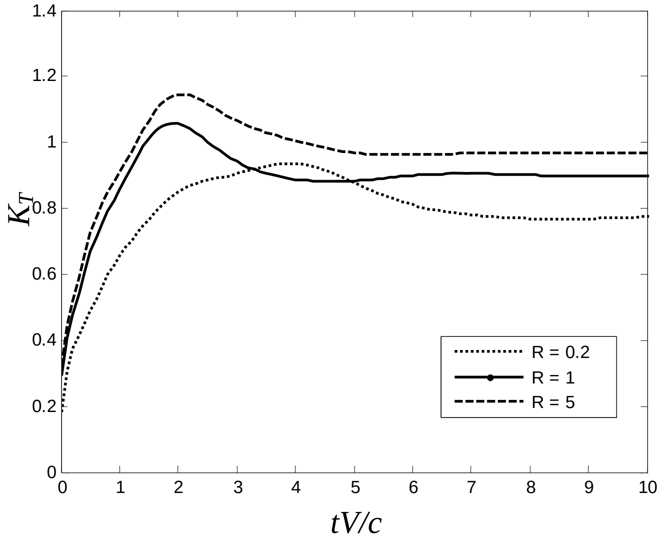

Figure 4. Normalized dynamic SIFs K_T vs normalized time for different material property $R = c_{44}^{e0} / \mu$ when $\beta = +1$

7. Conclusions

The dynamic fracture analysis of an interface crack between magnetoelectroelastic and functionally graded elastic layers under anti-plane shear and in-plane electric and magnetic impacts is performed using the integral transform method. The mixed-boundary-value problem of the interface crack is reduced to solving dual integral equations, which are further expressed in terms of Fredholm integral equations of the second kind. The asymptotic stress fields near the crack tip are obtained and the stress intensity factor is calculated. Crack propagation direction is predicted based on the maximum hoop stress intensity factor criterion, which shows that the crack will propagate along the extension of the original plane. Numerical results show that the SIFs are influenced by the geometric size ratios and the material properties of the magnetoelectroelastic composite. The obtained results are very useful for the safety and reliability design of the magnetoelectroelastic composite.

References

[1] C.W. Nan, Magnetoelectric effect in composites of piezoelectric and piezomagnetic phases. Phys Rev B, B50 (1994) 6082-6088.
[2] X. Wang, Z. Zhong, A circular tube or bar of cylindrically anisotropic magnetoelectroelastic material under pressuring loading. Int J Eng Sci, 41 (2003) 2143-2159.
[3] Z.F. Song, G.C. Sih, Crack initiation behavior in a magnetoelectroelastic composite under in-plane deformation. Theor Appl Fract Mech, 39 (2003) 189-207.

[4] C.F. Gao, K. Hannes, B. Herbert, Crack problems in magnetoelectroelastic solids. Part I: exact solution of a crack. Int J Eng Sci, 41 (2003) 969-981.
[5] B.L. Wang, Y.W. Mai, Fracture of piezoelectromagnetic materials. Mech Re Commu, 31 (2004) 65-73.
[6] Q.H. Qin, 2D Green's functions of defective magnetoelectroelastic solids under thermal loading. Eng Anal Bound Elem, 29 (2005) 577-585.
[7] X.F. Li, Dynamic analysis of a cracked magnetoelectroelastic medium under antiplane mechanical and inplane electric and magnetic impacts. Int J Solids Struct, 42 (2005) 3185-3205.
[8] K.Q. Hu, G.Q. Li, Electro-magneto-elastic analysis of a piezoelectromagnetic strip with a finite crack under longitudinal shear. Mech Mater, 37 (2005) 925-934.
[9] K.Q. Hu, G.Q. Li, Constant moving crack in a magnetoelectroelastic material under anti-plane shear loading. Int J Solids Struct, 42 (2005) 2823-2835.
[10] K.Q. Hu, Y.L. Kang, G.Q. Li, Moving crack at the interface between two dissimilar magnetoelectroelastic materials. Acta Mech, 182 (2006) 1-16.
[11] X.C. Zhong, X.F. Li, A finite length crack moving along the interface of two dissimilar magnetoelectroelastic materials. Int J Eng Sci, 44 (2006) 1394-1407.
[12] W.J. Feng, E. Pan, X. Wang, Dynamic fracture analysis of a penny-shaped crack in a magnetoelectroelastic layer. Int J Solids Struct, 44 (2007) 7955-7974.
[13] R. Rojas-Diaz, F. Garcia-Sanchez, A. Saez, C. Zhang, Fracture analysis of magnetoelectroelastic composite materials. Key Eng Mat, Advances in Fracture and Damage Mechanics VI, 348-349 (2007) 69-72.
[14] H.D. Yong, Y.H. Zhou, Transient response of a cracked magnetoelectroelastic strip under anti-plane impact. Int J Solids Struct, 44 (2007) 705-717.
[15] K.Q. Hu, Q.H. Qin, Y.L. Kang, Anti-plane shear crack in a magnetoelectroelastic layer sandwiched between dissimilar half spaces. Eng Fract Mech, 74 (2007) 1139-1147.
[16] Z.G. Zhou, Z.T. Chen, Fracture mechanics analysis of a partially conducting mode I crack in piezoelectromagnetic materials. Eur J Mech-A Solid, 27 (2008) 824-846.
[17] B.L. Wang, J.C. Han, Effect of Finite Cracking on the Magneto-electric Coupling Properties of Magneto-electro-elastic Composite Laminates. J Intel Mat Syst Str, 21 (2010) 1669-1679.
[18] K.Q. Hu, Z.T. Chen, Pre-curving analysis of an opening crack in a magnetoelectroelastic strip under in-plane impact loadings. J Appl Phys, (2012) In Press.
[19] K.Q. Hu, Z.T. Chen, Dynamic response of a cracked magnetoelectroelastic layer sandwiched between two elastic layers. ZAMM Z Angew Math Mech, DOI 10.1002/zamm.201200105.
[20] Y.P. Wan, Y.P. Yue, Z. Zhong, Z., The mode III crack crossing the magnetoelectroelastic bimaterial interface under concentrated magnetoelectromechanical loads. Int J Solids Struct, 49 (2012) 3008-3021.
[21] G.R. Buchanan, Layered versus multiphase magneto-electro-elastic composites. Compos Part B, 35 (2004) 413-420.